Vol 17 No 11, November 2008
1674-1056/2008/17(11)/4285-07

Chinese Physics B

© 2008 Chin. Phys. Soc.
and IOP Publishing Ltd

Excitonic optical absorption in semiconductors under intense terahertz radiation*

Zhang Tong-Yi(张同意)† and Zhao Wei(赵 卫)

State Key Laboratory of Transient Optics and Photonics, Xi'an Institute of Optics and Precision Mechanics, Chinese Academy of Sciences, Xi'an 710119, China

(Received 16 April 2008; revised manuscript received 16 June 2008)

The excitonic optical absorption of GaAs bulk semiconductors under intense terahertz (THz) radiation is investigated numerically. The method of solving initial-value problems, combined with the perfect matched layer technique, is used to calculate the optical susceptibility. In the presence of a driving THz field, in addition to the usual exciton peaks, 2p replica of the dark 2p exciton and even-THz-photon-sidebands of the main exciton resonance emerge in the continuum above the band edge and below the main exciton resonance. Moreover, to understand the shift of the position of the main exciton peak under intense THz radiation, it is necessary to take into consideration both the dynamical Franz–Keldysh effect and ac Stark effect simultaneously. For moderate frequency fields, the main exciton peak decreases and broadens due to the field-induced ionization of the excitons with THz field increasing. However, for high frequency THz fields, the characteristics of the exciton recur even under very strong THz fields, which accords with the recent experimental results qualitatively.

Keywords: exciton, optical absorption, terahertz radiation, dynamical Franz–Keldysh effect
PACC: 7135, 7110, 4225B

1. Introduction

The effect of external electric fields on the optical absorption near the band edge in semiconductors is a subject that has been extensively studied both theoretically and experimentally. The resulting shift and broadening of the band edge absorption by an electric field in bulk semiconductors is well known as the Franz–Keldysh effect (FKE).[1−4] However, to model the electro-absorption at low temperatures appropriately, one must also include the excitonic effects,[5,6] because the excitonic effects in quantum-well structures are much more pronounced and can be clearly observed even at room temperature.[7−11] And the effect of electric fields on excitonic absorption in quantum wells has been widely used as an electro-optical modulation in modern optical communications. Therefore, there are a great many of papers dealing with the excitonic optical absorption of low-dimensional semiconductor structures, and some excellent monographs have already been available.[12,13] The FKE was also generalized to the case of an ac electric field, i.e. dynamical Franz–Keldysh effect (DFKE), by Yacoby,[14] Rebane,[15] and recently by Jauho and Johnsen[16], and Johnsen and Jauho.[17] Since terahertz (THz) radiation and its effect on the transport and the optical properties have attracted much attention in recent years,[18−29] the THz DFKE in low-dimensional semiconductor structures has been investigated, without[16,17] and with[30−40] the Coulomb interaction included. However, for three-dimensional bulk semiconductors, there are few reports on the numerical study of the DFKE, and the reported results for bulk semiconductors were presented only for free electron–hole absorption, with the Coulomb interaction neglected.[41]

In this paper, we extend the real space initial-value method[42−44] to time-dependent field and investigate the DFKE of excitonic optical absorption in a bulk semiconductor under intense THz radiation. The theoretical approach is based on the discretization of the Hamiltonian in real space and the solution of the initial-value problem in real time. This approach, combined with the perfect matched layer

*Project supported by the National Natural Science Foundation of China (Grant No 60777017), the National Basic Research Program of China (Grant No 2007CB310405), China Postdoctoral Scientists Foundation (Grant No 20060390323), and K. C. Wong Education Foundation, Hong Kong, China.
†E-mail: tyzhang@opt.ac.cn

(PML) technique developed for Schrödinger-like equations, can significantly improve the efficiency of the calculations. This paper is also stimulated by a series of recent optical absorption experiments in bulk semiconductors.[45−48] In addition to the generation of THz-sidebands of mid-infrared light, the experiments also show the absence of exciton quenching in the presence of strong THz fields at high frequencies, which is not well explained.[47] The results presented in this paper show that this is due to the adiabatic stabilization of excitons in a high frequency field, acting as the strong-field atomic stabilization.[49,50]

2. General theory

The linear optical absorption coefficient $\alpha(\omega)$ of dielectric media is proportional to the imaginary part of the linear optical susceptibility $\chi(\omega)$ as given

$$\alpha(\omega) = \frac{\omega}{cn}\mathrm{Im}\chi(\omega), \tag{1}$$

where c is the speed of light in vacuum, n is the refractive index of the dielectric media. The linear optical susceptibility relates the exciting optical field $E(t)$ to the induced macroscopic polarization $P(t)$ through

$$P(t) = \int_{-\infty}^{t} \mathrm{d}t' \epsilon_0 \chi(t,t') E(t'), \tag{2}$$

where ϵ_0 is the dielectric constant of free space. By performing a Fourier transform, one obtains the linear optical susceptibility as

$$\chi(\omega) = \frac{\tilde{P}(\omega)}{\epsilon_0 \tilde{E}(\omega)}. \tag{3}$$

The macroscopic polarization in a semiconductor is related to the microscopic electron–hole pair amplitude $\psi(\boldsymbol{r}_\mathrm{e}, \boldsymbol{r}_\mathrm{h}, t)$ by

$$P(t) = \frac{1}{V} d^* \int \mathrm{d}^3 \boldsymbol{r} \psi(\boldsymbol{r}, \boldsymbol{r}, t), \tag{4}$$

where V is the normalization volume, and d^* is the complex conjugate of the dipole matrix element d between valence band and conduction band. To determine the microscopic electron–hole pair amplitude, we solve the time-dependent inhomogeneous Schrödinger equation

$$\mathrm{i}\hbar \frac{\mathrm{d}\psi(t)}{\mathrm{d}t} = \hat{H}\psi(t) - \mathrm{i}\hbar\gamma\psi(t) - d\delta(\boldsymbol{r}_\mathrm{e} - \boldsymbol{r}_\mathrm{h})E(t), \tag{5}$$

where $\hbar$ is Planck constant, γ is a phenomenological dephasing constant, $\hat{H}$ is the Hamiltonian of the electron–hole pair system. In fact, this is the polarization equation of the semiconductor Bloch equations in real-space and in the low-density limit. Usually, $E(t)$ is the slowly varying envelop of the excitation optical pulse, and Eq.(5) is used extensively for studying the transient optical response of photoexcited semiconductors and the motion of polarization wave packet in real space.[36] In that case, the initial condition of the polarization is zero everywhere in the calculated region, while in the initial problem scheme introduced by Glutsch *et al*[42] the excitation optical pulse is set to be in a specific form, i.e. Dirac delta function, $E(t) = -\mathrm{i}\hbar\delta(t)$, and the problem is further converted into the initial case, i.e. initially, the polarization is zero everywhere except at the origin, where the value of polarization is set to be d. And expression (3) becomes

$$\begin{aligned}\chi(\omega) =& \frac{1}{\epsilon_0}\tilde{P}(\omega) \\ =& \lim_{T\to\infty} \int_0^T \mathrm{d}t \mathrm{e}^{\mathrm{i}\omega t} \mathrm{e}^{-\gamma t} P(t)/\epsilon_0.\end{aligned} \tag{6}$$

In this paper, we investigate the DFKE of bulk semiconductors by using the initial-value problem method, due to its high storage efficiency and numerical effectiveness and nonperturbatively dealing with the driven THz field. The Hamiltonian of a bulk exciton under a THz electric field is given by

$$\begin{aligned}\hat{H} =& -\frac{1}{2m_\perp}\frac{1}{\rho}\frac{\partial}{\partial\rho}\left(\rho\frac{\partial}{\partial\rho}\right) - \frac{1}{2m_\parallel}\frac{\partial^2}{\partial z^2} \\ & - \frac{e^2}{4\pi\epsilon_0\epsilon\sqrt{\rho^2+z^2}} + eF(t)z,\end{aligned} \tag{7}$$

where $m_\perp$ and $m_\parallel$ are the reduced longitudinal (perpendicular to the field direction) mass and the transverse (parallel to the field direction) mass, respectively; z and ρ are the relative distances between the electron and the hole along the THz field direction and in the perpendicular plane, respectively; e is the elementary charge; ϵ is relative dielectric constant; $F(t) = F_0\cos(\Omega t - \phi)$ is the applied THz field with F_0, Ω, and ϕ the strength, frequency, and initial phase of the THz electric field, respectively. The first term on the right-hand side in Eq.(7) describes the kinetic energy in the plane perpendicular to the field direction, the second term represents the kinetic energy along the field direction, the third term refers to the Coulomb interaction between an electron and a hole, and the last term describes the effect of the THz electric field. In our calculation, Hamiltonian

(7) is discretized by the finite-difference scheme for differential operators, while the Coulomb potential is discretized by employing the ground-state-adapted discretization.[42,51] Since ground-state wave function and energy are related through, $-\frac{1}{2}\sum_{j'} \Delta_{jj'} \Phi_{\mathrm{gs};j'} - V_j \Phi_{\mathrm{gs};j} = E_{\mathrm{gs}} \Phi_{\mathrm{gs};j}$, the discretized potential is

$$-V_j = E_{\mathrm{gs}} + \frac{1}{2}\frac{\sum_{j'} \Delta_{jj'} \Phi_{\mathrm{gs};j'}}{\Phi_{\mathrm{gs};j}}. \tag{8}$$

It has been shown that this method gives practical results even better than those obtained by using the finite element method and reduces the programming effort. The delta function $\delta(r)$ is discretized as

$$\bar{\delta}_{j0} = \frac{4}{\pi(\Delta\rho)^2(\Delta z)}\delta_{j0}. \tag{9}$$

It could be confirmed by the relation of $2\pi \int_0^{\Delta\rho/2} \rho \mathrm{d}\rho \int_{-\Delta z/2}^{\Delta z/2} \mathrm{d}z \bar{\delta}_{j0} = 1$.

A major progress in solving the wave equations of electromagnetism and quantum mechanics in real space is the introduction of absorbing boundary conditions, which leads to a significant reduction in both memory and numerical effort. The introduction of absorbing boundary condition is to simulate wave propagation in an infinite domain by suppressing the reflection of the wavepackets at the artificial boundaries. The PML technique is an effective and convenient absorbing boundary condition technique and has been widely used in electromagnetic finite difference time domain (FDTD) simulation.[52,53] The idea of absorbing boundary conditions in quantum mechanic calculation lies in the modifying of the Hamiltonian or the boundary conditions. This can be done by modifying the potential or the operator of the kinetic energy. Ahland *et al*[54] have proposed an PML technique and demonstrated its usefulness for the calculation of the optical absorption in the presence of continuum states. The PML is realized by introducing complex stretched coordinates. Recently, Glutsch *et al*[55] demonstrated the PML by using complex effective masses in the ideal absorbing layers and calculated the optical absorption of a superlattice in the regime of the Zener breakdown. Candidates for absorbing boundary conditions are suggested for those directions, where (i) the initial wavepacket is localized near the origin, (ii) the polarization of interest is only in a small region around the origin, and (iii) the potential approaches a constant far from the origin so that the time evolution of polarization is the same as that for a free particle.[13] In this paper, we use the complex effective mass formulation. Thus, the Hamiltonian of kinetic energy becomes

$$\hat{H} = -\frac{\partial}{\partial z}\frac{1}{2m(z)}\frac{\partial}{\partial z}. \tag{10}$$

This expression is in a typical form of a Hamiltonian when the mass of the particle depends on the coordinate. However, in the present case, the coordinate-dependent mass is complex. The usefulness of the complex effective mass is twofold: the increasing of the real part causes a reduction in reduces wavelength for a fixed energy and the imaginary part leads to the damping of the wave packet. The mass is chosen as

$$\begin{aligned} &m(z) = 1, \quad \text{for} \quad |z| \leqslant \frac{L_1}{2}; \\ &m(z) \to |\infty| \mathrm{e}^{\mathrm{i}\alpha} \quad \text{for} \quad z \to \pm\frac{L_2}{2};\ 0 < \alpha < \pi, \end{aligned} \tag{11}$$

where L_1 and L_2 are the boundary of the PML and the computed domain respectively. As the spectrum is practically independent of the specific form of the complex effective mass, we adopt the following expression that was used by Glutsch[13]

$$m(z) = \begin{cases} 1, & |z| \leq L_1, \\ 1 + \mathrm{i}\left[\sec\left(\frac{\pi}{2}\frac{|z| - L_1}{L_2 - L_1}\right) - 1\right], & L_1 < |z| < L_2. \end{cases} \tag{12}$$

Through this modification, we can significantly reduce the computed domain.

3. Numerical results and discussions

To simplify the numerical calculations and improve the numerical accuracy, we use excitonic Hartree units, which set all quantities to be of the order of unity. The units for energy (E), length (a), time (t), and electric field (F) are 2Ry*, a_{B}^*, $\hbar/2\mathrm{Ry}^*$, and $2\mathrm{Ry}^*/ea_{\mathrm{B}}^*$ respectively, and for GaAs parameters, their values are 9.37 meV, 11.7 nm, 70.3 fs, and

7.98 kV/cm, respectively.[13] Here, Ry* and a_B^* are the excitonic Rydberg constant and the Bohr radius, respectively. Thus, the bound energy of bulk exciton is 0.5 in the units. In all figures throughout this paper, the zero of the energy is the gap energy at zero temperature. And the curves are offset for clarity.

Although the free electron–hole pair interband absorption is never realized in reality, it is still of theoretical interest, for it shows the optical density of states and allows one to clearly identify the role of excitonic effects. In Fig.1, we show the free electron–hole pair interband absorption under a THz field with different initial phases. This is calculated by simply neglecting the Coulomb interaction term in Eq.(7). The dashed line represents the optical absorption of a free electron–hole pair in the absence of the THz field, and the upmost solid line refers to the optical absorption of a phase-averaged free electron–hole pair in the presence of the THz field. By comparing these spectra, we find that the principal effect of the THz field on the spectrum occurs in the vicinity of the absorption edge. The effect of the THz field is responsible for the dynamical Franz–Keldysh blueshift of the absorption edge of the ponderomotive energy $E_K = (eF)^2/(4m\Omega^2)$ (0.77 in our parameters), as well as the enhanced absorption below and reduced absorption above the unshifted bandedge. These features are in consistent with the results observed in recent experiments for bulk semiconductors.[45,48] Figure 1 also

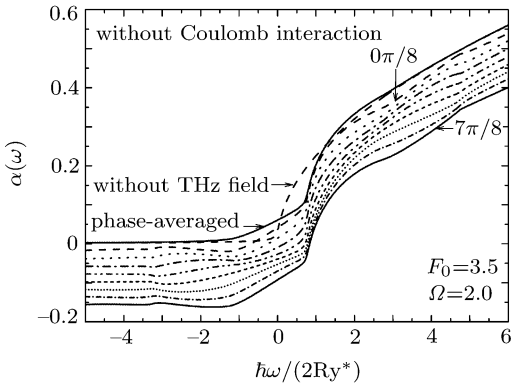


Fig.1. Optical absorption spectra of free electron–hole pairs in a bulk GaAs semiconductor under THz radiation. (excitonic Hartree units are used.) The dashed line is for the absorption spectrum in the absence of the THz field, the upmost solid line is for the phase-averaged absorption spectrum in the presence of the THz field, the other solid lines from up to down correspond to the absorption spectrum in the presence of the THz field with different initial phases from $0\pi/8$ to $7\pi/8$.

shows the dependence of the absorption spectrum on the initial phase of the THz field. The lines below the upmost line correspond to the initial phase of the THz field of $0\pi/8$-to-$7\pi/8$ from the top to the bottom in steps of $1\pi/8$. The absorption spectrum is slightly distorted and modulated at every multiple of the THz-photon energy. However, these features become smoothed down for the phase-averaged spectrum.

In Fig.2, we show the optical absorption spectra of a bulk GaAs driven by a THz electric field, with the excitonic effect included. Figure 2(a) depicts the optical absorption spectrum under a THz field with a frequency of 0.4 and a strength of 0.3. Apart from the Rydberg series of *s*-symmetric excitons below the band gap and a continuum above the band gap for undriven bulk semiconductors, a few prominent and intriguing features show up, which have been identified as 2p replicas and two- and even four-THz-photon sidebands of 1s exciton and labelled in Fig.2(a) for clarity. The absence of the odd photon sidebands is due to the inversion symmetry of the consider system. Though these main features have been predicted for quantum wells based on the Green function techniques, four-THz-photon sideband and the 2p replica above the band edge, and two-THz-photon sideband below the 1s exciton peak are not identified there because of the selected base functions in the calculations.[31] Figure 2(b) and 2(c) show the field strength dependences of the absorption spectrum at THz field frequencies of 0.4 and 0.5, slightly less and larger than the 1s-to-2p resonance frequency, respectively. With field strength increasing, for the frequency of 0.4, the main 1s exciton peak initially experiences redshifts and then blueshifts, while for the frequency of 0.5, the main 1s exciton peak blueshifts always. These phenomena have indeed been observed experimentally in quantum wells and first explained by considering the interplay between the ac Stark effect (which results in a redshift for $\Omega <$ 1s $\longrightarrow$ 2p but a blueshift for $\Omega >$ 1s $\longrightarrow$ 2p) and DFKE (which results in net blueshift).[30] With field strength increasing, the 1s and the 2s exciton peaks decrease in height and broaden, meanwhile the sidebands become more prominent. When the field strength becomes comparable with the bound energy of exciton, the exciton peaks, the replica, and the sidebands broaden significantly and eventually merge (because the field can cause the ionization of exciton), thus the details become gradually indistinguishable.

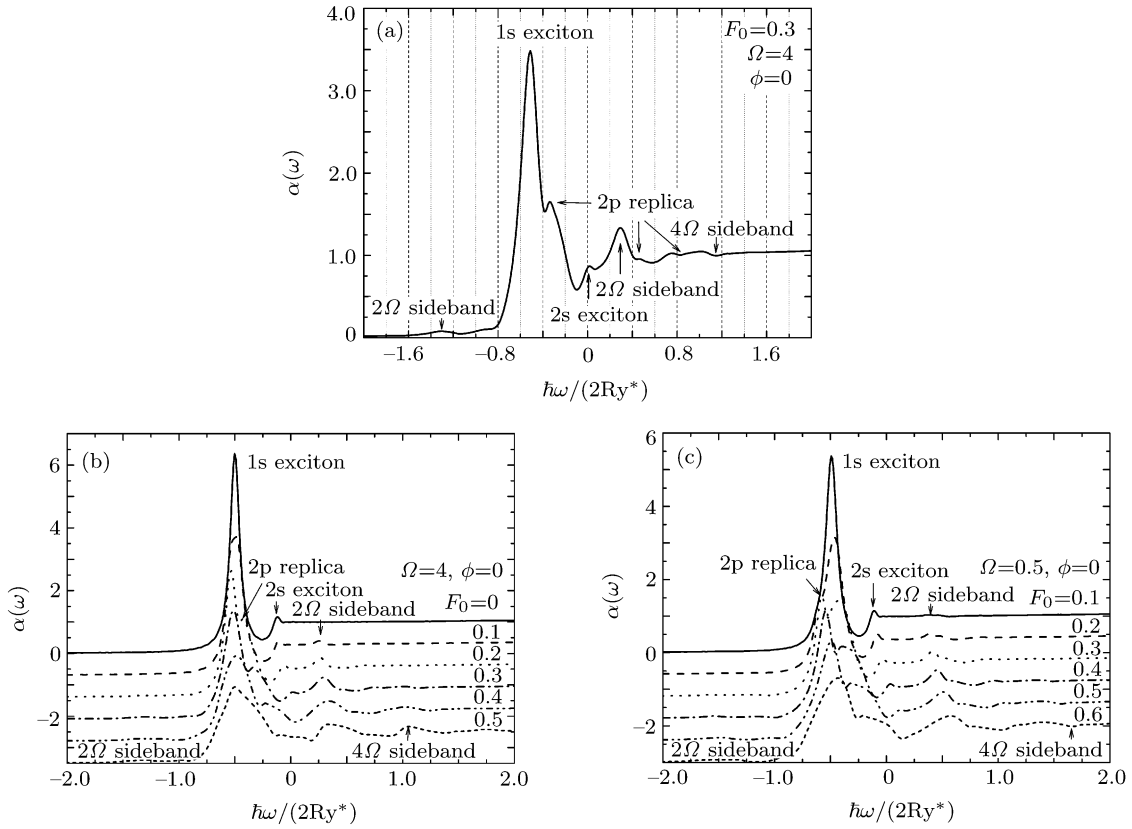


Fig.2. Optical absorption spectra of a THz-field-driven bulk GaAs semiconductor. (a) The frequency, the strength, and the initial phase of the THz field are 0.4, 0.3 and 0, respectively. The dependence of the optical absorption on the strength of the THz field are shown with frequencies of 0.4 (b) and 0.5 (c), which are slightly less and larger than the 1s-to-2p resonance frequency, respectively. The field strength varies from top to bottom in steps of 0.1.

We show the optical absorption spectrum under a strong and high-frequency THz field in Fig.3. In Fig.3(a), we show the optical absorption of the bulk semiconductor under THz field at a frequency Ω of 1 with the field strength increasing from 0.5 to 3.5 (much larger than the bound energy of excitons). With the THz field strength increasing, more and more sidebands and replicas emerge, and the heights of the one-THz-photon 2p replica below main exciton peak increase and become comparable with and dominant over the reduced main exciton peak. Eventually, with the field strength increasing further, the optical absorption spectra become similar to those of the free electron–hole pairs with modulation by the replicas and sidebands. This is due to the ionization of excitons by the THz field. However, when the frequency of the field further increases to 2, the optical absorption spectra change drastically as shown in Figs.3(b) and 3(c). Though the field strength is much larger than the bound energy of the excitons, which is expected to cause the ionization of these excitons, the features of the excitons (even the 2s exciton) recur in this high-frequency region. Apart from the significant blueshifts, the features of excitons, such as 1s and 2s exciton peaks, 2p replicas, two-THz-photon sidebands, all recur evidently. Thus, we demonstrate theoretically the exciton surviving phenomena under strong and high-frequency fields as reported in the recent experiments.[46,47] We attribute this recurrence of excitonic characteristics in strong fields at high-frequencies to the adiabatic stabilization of excitons in high frequency fields,[49] which acts as the strong-field atomic stabilization.[50] Since, in practice, the transient optical absorption experiments are performed with a femtosecond laser pulse, which is much less than the period of the driving THz field, we expect that the spectra may be dependent on the phase of the THz field at which the femtosecond pulse arrives. Figure 2(c) shows the dependence of the absorption spectrum on the phase of the THz field. The upmost trace corresponds to the phase-averaged spectrum, and the eight traces below this trace, from up to down, cor-

respond to the initial phase of $0\pi/8$ to $7\pi/8$. We see the main 1s and 2s exciton peaks, as well as the 2p replica below them, are nearly insensible to the phase, while two-THz-photon replicas of 1s and 2s exciton, as well as 2p replica above band edge are sensitive to the phase. This is why the two-THz-photon sidebands of main exciton peak above the bandedge in Figs.2(a) and 2(b) are dips, where the initial phase of the THz field is set to be zero. However, the phase-averaged spectrum becomes featureless in the vicinity of the phase-sensitive features due to their cancellation on averaging the phase.

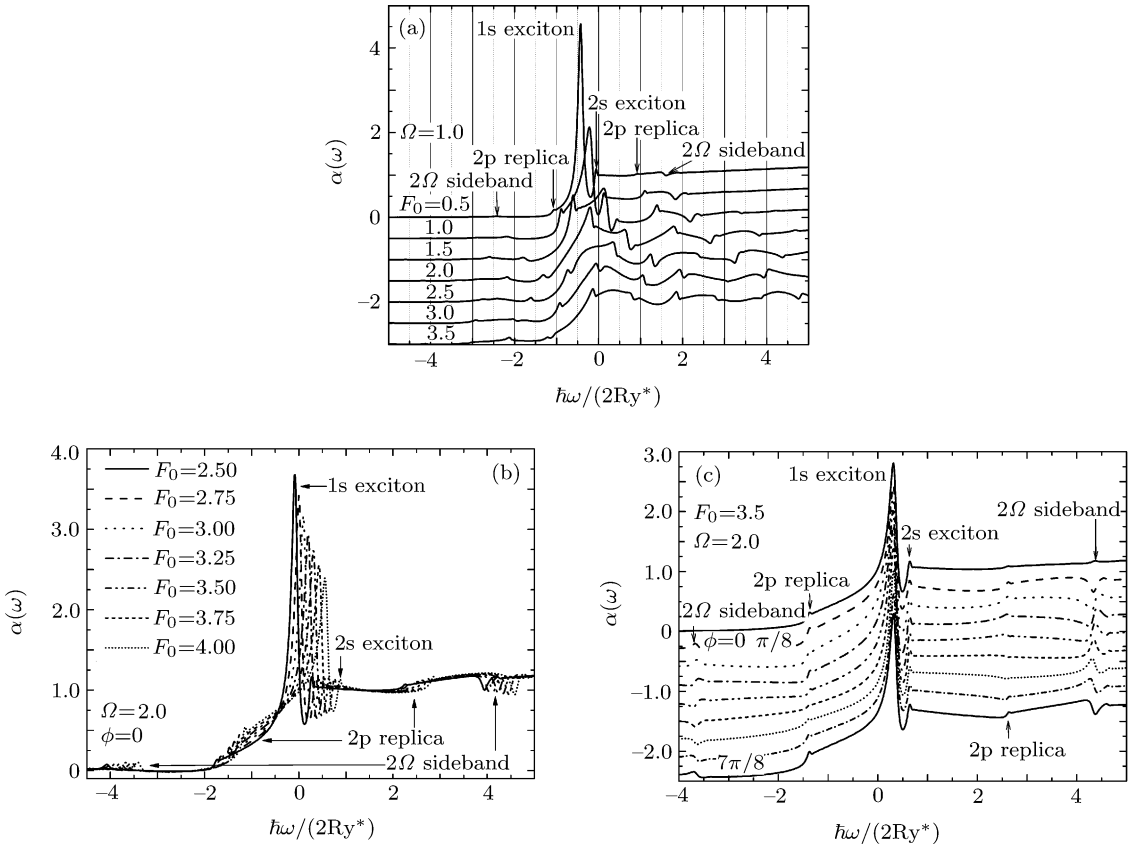


Fig.3. Optical absorption spectra of a THz-field-driven bulk GaAs semiconductor with higher frequencies, showing the dependences of the optical absorption on the strength of the THz field with frequencies of 1(a) and 2(b), respectively, and the dependence of the optical absorption on the initial phase of the THz field, with field strength and frequency fixed (c) at 3.5 and 2 respectively.

4. Conclusions

We have performed the numerical study the DFKE on excitons in bulk GaAs semiconductors. By employing the method of initial-value solution and PML technique in real-space, the external electric field and Coulomb interaction have been included nonperturbatively in the numerical scheme. In the presence of a THz electric field, the optical spectrum exhibits rich fine structures due to the emergence of the 2p replicas of the dark 2p exciton and even-number-THz-photon sidebands. The numerical results also show that the excitonic characteristics, as well as the THz-field-induced effect recur in high frequency THz fields, even though the field strengths are far beyond the bound energies of the excitons. The recurrence of excitonic characteristics can be attributed to the adiabatic stabilization of excitons under intense and high-frequency fields.

References

[1] Franz W Z 1958 *Naturforsch* **13**a 484
[2] Keldysh L V 1958 *Zh. Eksp. Teor. Fiz.* **34** 1118 [1958 *Sov. Phys.-JETP* **34** 788]
[3] Pedersen T G and Lynge T B 2002 *Phys. Rev.* B **65** 085201
[4] Garcia H 2006 *Phys. Rev.* B **74** 035212
[5] Vrehen Q H F 1968 *J. Phys. Chem. Solids* **29** 129
[6] Dow J D and Redfield D 1970 *Phys. Rev.* B **1** 3358
[7] Miller D A B, Chemla D S, Eilenberger D J, Smith P W, Gossard A C and Wiegmann W 1983 *Appl. Phys. Lett.* **42** 925
[8] Kirchoefer S W, Holonyak N, Hess K, Gulino D A, Drickamer H G, Coleman J J and Dapkus P D 1984 *Appl. Phys. Lett.* **42** 821
[9] Weiner J S, Chemla D S, Miller D A B, Wood T H, Sivco D and Cho A Y 1985 *Appl. Phys. Lett.* **46** 619
[10] Miller D A B, Chemla D S, Damen T C, Gossard A C, Wiegmann W, Wood T H and Burrus C A 1984 *Phys. Rev. Lett.* **53** 2173
[11] Miller D A B, Chemla D S, Damen T C, Gossard A C, Wiegmann W, Wood T H and Burrus C A 1985 *Phys. Rev.* B **32** 1043
[12] Haug H and Koch S W 2004 *Quantum Theory of the Optical and Electronic Properties of Semiconductors* 4th edn (Singapore: World Scientific)
[13] Glutsch S 2004 *Excitons in Low-Dimensional Semiconductors* (Berlin: Springer)
[14] Yacoby Y 1968 *Phys. Rev.* **169** 610
[15] Rebane Y T 1985 *Sov. Phys. Solid State* **27** 824
[16] Jauho A P and Johnsen K 1996 *Phys. Rev. Lett.* **76** 4576
[17] Johnsen K and Jauho A P 1998 *Phys. Rev.* B **57** 8860
[18] Cao J C 2003 *Phys. Rev. Lett.* **91** 237401
[19] Zhang T Y and Cao J C 2004 *Chin. Phys.* **13** 1742
[20] Meng T H, Zhao G Z and Zhang C L 2008 *Acta Phys. Sin.* **57** 3846 (in Chinese)
[21] Wu B H and Cao J C 2006 *Phys. Rev.* B **73** 245412
[22] Wu B H and Cao J C 2006 *Phys. Rev.* B **73** 205318
[23] Sun H Q, Zhao G Z, Zhang C L and Yang G Z 2008 *Acta Phys. Sin.* **57** 790 (in Chinese)
[24] Wang C and Cao J C 2005 *Phys. Rev.* B **72** 045339
[25] Yan W, Yang Y P, Chen H and Wang L 2007 *Phys. Rev.* B **75** 085323
[26] Ma M R, Chen Y L and Wang C 2006 *Chin. Phys.* **15** 2657
[27] Zhang X B and Shi W 2006 *Acta Phys. Sin.* **55** 5237 (in Chinese)
[28] Wu H C, Sheng Z M, Dong Q L, Xu H and Zhang J 2007 *Phys. Rev.* E **75** 016407
[29] Zhang Y H and Wang C 2006 *Chin. Phys.* **15** 649
[30] Nordstrom K B, Johnsen K, Allen S J, Jauho A P, Birnir B, Kono J, Noda T, Akiyama H and Sakaki H 1998 *Phys. Rev. Lett.* **81** 457
[31] Johnsen K and Jauho A P 1999 *Phys. Rev. Lett.* **83** 1207
[32] Hughes S and Citrin D S 1999 *Phys. Rev.* B **59** R5288
[33] Citrin D S and Hughes S 2000 *Phys. Rev.* B **61** R5105
[34] Hughes S and Citrin D S 2000 *Phys. Rev. Lett.* **84** 4228
[35] Hughes S 2001 *Phys. Rev.* B **63** 153308
[36] Hughes S 2004 *Phys. Rev.* B **69** 205308
[37] Zhang T Y and Cao J C 2004 *J. Phys.: Condens. Matter* **16** 9093
[38] Zhang T Y, Zhao W, Cao J C and Qasim G 2005 *J. Appl. Phys.* **98** 094311
[39] Zhang T Y and Zhao W 2006 *Phys. Rev.* B **73** 245337
[40] Zhang T Y, Zhao W, Liu X M and Zhang C 2007 *Appl. Phys. Lett.* **91** 041909
[41] Xu W 2006 *Appl. Phys. Lett.* **89** 171107
[42] Glutsch S, Chemla D S and Bechstedt F 1996 *Phys. Rev.* B **54** 11592
[43] Zhang T Y, Zhao W, Zhu H Y, Zhu S L and Liu X M 2006 *Chin. Phys.* **15** 2151
[44] Zhang T Y and Zhao W 2008 *Europhys. Lett.* **82** 67001
[45] Chin A H, Bakker J M and Kono J 2000 *Phys. Rev. Lett.* **85** 3293
[46] Chin A H, Calderón O G and Kono J 2001 *Phys. Rev. Lett.* **86** 3292
[47] Chin A H, Kono J and Solomon G S 2002 *Phys. Rev.* B **65** 121307(R)
[48] Srivastava A, Srivastava R, Wang J and Kono J 2004 *Phys. Rev. Lett.* **93** 157401
[49] Liu R B and Zhu B F 2002 *Phys. Rev.* B **66** 033106
[50] Popov A M, Tikhonova O V and Volkova E A 2003 *J. Phys.* B: *At Mol. Opt. Phys.* **36** R125 and references therein
[51] Siarkos A, Runge E and Zimmermann R 2000 *Phys. Rev.* B **61** 10854
[52] Berenger J P 1994 *J. Comput. Phys.* **114** 185
[53] Sullivan D M 2000 *Electromagnetic Simulation Using the FDTD Method* (New York: IEEE Press)
[54] Ahland A, Schulz D and Voges E 1999 *Phys. Rev.* B **60** R5109
[55] Glutsch S, Bechstedt F, Rosam B and Leo K 2001 *Phys. Rev.* B **63** 085307